S. Afr. J. mar. Sci. 21: 99–115
1999

SYNOPTIC ENVIRONMENT OF COMPOSITE TROPICAL CYCLONES IN THE SOUTH-WEST INDIAN OCEAN

*B. A. PARKER** and *M. R. JURY* †

The composite structure of the tropical cyclone (TC) environment in the South-West Indian Ocean is analysed using European Community medium-range weather data. Conditions suitable for the development of tropical cyclones are present between 5 and 15°S and between 40 and 100°E. Groups of westward-moving and poleward-recurving TCs are used to construct system-following composites from three days before maximum intensity to one day after. The synoptic fields surrounding the westward-moving composite TC remain steady, whereas the recurving composite environment supports rapid vortex growth. Interaction with a subtropical trough is prominent in the recurving TC. The results offer useful insights to weather interactions in the South-West Indian Ocean.

The meteorology of the South-West (SW) Indian Ocean (Fig. 1a) has only recently been studied on a scale comparable to that undertaken for other ocean basins, mainly as a result of greater interest in the Indian northern summer monsoon and the low economic status of the island countries of the region (Jury 1993). Because of sparsity of data, SW Indian Ocean tropical cyclone (TC) climatology is limited to estimates of tracks, intensity, and overall frequency. Only two radiosonde stations operate in the cental tropics, namely Antananarivo, in central Madagascar, and Diego Garcia (4°S, 73°E), despite the recognized importance of that area in modulating the regional climate (Pathack 1993). Detailed aircraft surveys on the structure and dynamics of TCs have not been attempted there. This research is aimed at improving understanding by studying the atmospheric envelope surrounding TCs in the area between 5 and 30°S and between 50 and 90°E, using numerical weather model-interpolated meteorological fields.

Past studies of climate and weather variability over the tropical SW Indian Ocean have been limited in scope with regard to the region's atmospheric circulation and synoptic scale variability (Hastenrath 1985). Adjustments in the austral summer monsoon circulation have been shown to drive rainfall variations over Mauritius (Dennet 1978, Padya 1989), Madagascar (Williams 1990) and southern Africa (Walker 1989, Jury 1992). The presence of a climatic dipole for rainfall and outgoing longwave radiation (OLR) has been recorded between southern Africa and the SW Indian Ocean (Jury and Pathack 1991). The climatic dipole was concluded to be a regional response to the global *El Niño*-Southern Oscillation (ENSO) phenomena, and governs a large portion of interannual variability of summer convection (Jury 1992).

The irregularity and poor resolution of conventional observations have deterred many scientists from studying this region intensively. Ship-borne, international studies have been carried out, such as the International Indian Ocean Expedition in the early 1960s and more recently as part of the World Ocean Circulation Experiment. The low-level wind over the Indian Ocean (Fig. 1b) exhibits a broad region of convergence in the tropics north of Mauritius, as well as a centre of convergence near Madagascar. Regions of surface divergence occur in the trades south of Mauritius during most months (Padya 1989). The overlapping of weak, upper easterly shear and warm sea surface temperatures (SSTs) condusive to easterly wave, monsoon vortex and TC genesis occur in a narrow band from 10 to 15°S within the SW Indian Ocean (Riehl 1979, Anyamba *et al.* 1982, Arkin *et al.* 1986). Martin *et al.* (1993) found a zonal cloud band just south of the equator in the Indian Ocean, extending from Sumatra to the Moçambique Channel. The boundary between the tropical and subtropical maritime airmasses seldom advances south of 15°S, coinciding with the mean southern limit of the 28°C SST isotherm (Fig. 1a). Farther south, subtropical westerly flow above 500 hPa reduces the potential for development and maintenance of TCs (Padya 1989) and consequently affects their frequency, intensity and regional impact (Jury and Pathack 1991). The island of Mauritius is located centrally in the region of study and long-term rainfall records from there are of high quality. Therefore, its rainfall data can be used to define the period in which the SW Indian Ocean region experiences maximum atmospheric convection. From December to April the respective monthly levels of rainfall are 160, 235,

* South African Weather Bureau, Private Bag X097, Pretoria 0001, South Africa. E-mail: parker@cirus.sawb.gov.za
† Department of Geography, University of Zululand, Private Bag X001, Kwa-Dlangezwa 3886, South Africa E-mail: mjury@pan.uzulu.ac.za

Manuscript received: December 1997

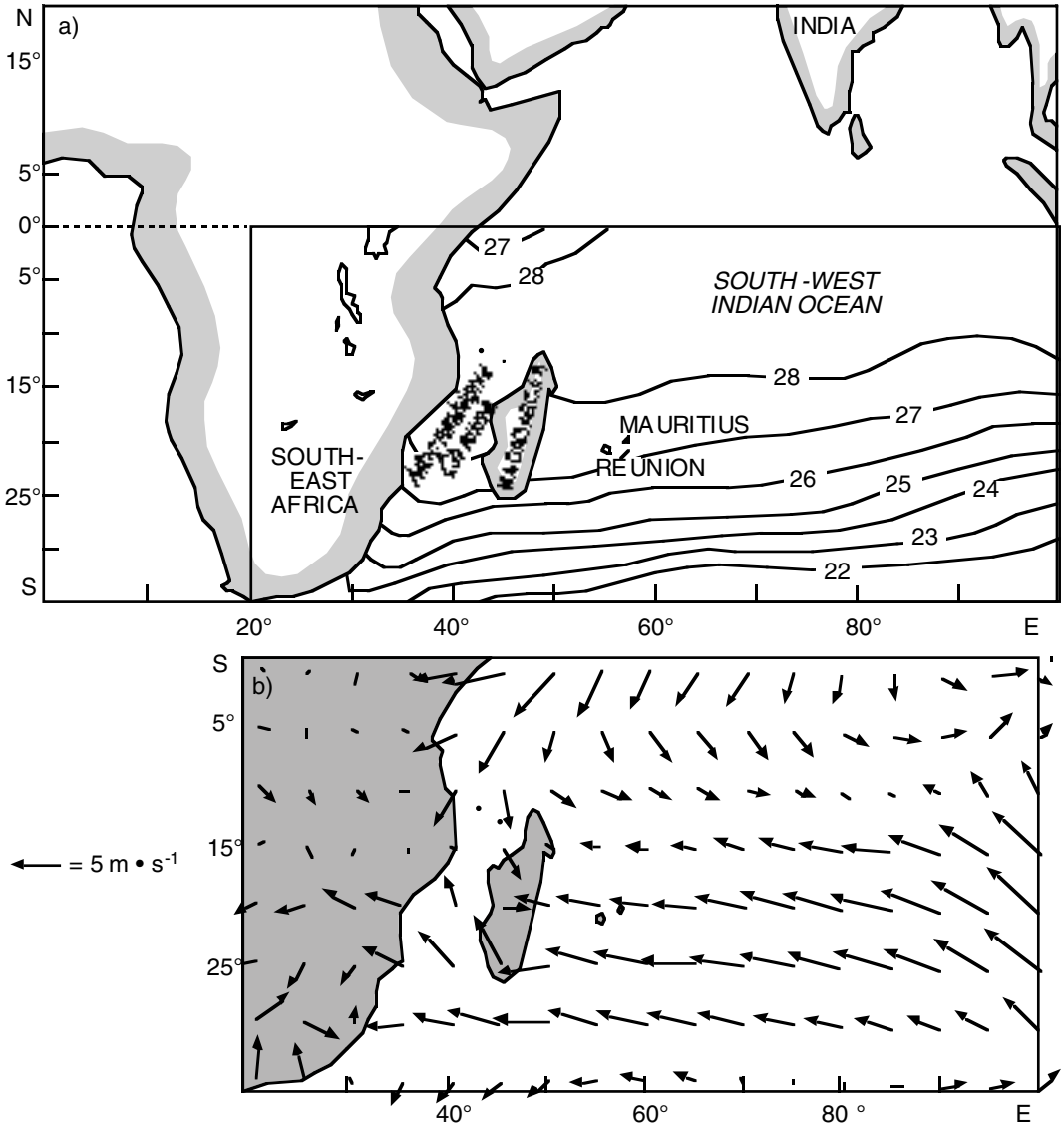

Fig. 1: Location of the study area, showing (a) mean SSTs during February (historical mean for the period 1950–1992, after Jury and Pathack 1991) and (b) mean surface wind vectors for the period December–March, 1987–1992

232, 190 and 170 mm, mostly contributed by TC events.

In a study on climatological associations with TCs of the SW Indian Ocean, Jury (1993) found that the 30-hPa quasi-biennial oscillation (QBO) modulated their occurrence (more TCs in the east phase), in contrast to that found by Gray (1984) for the North Atlantic. A poor correlation was found with the global ENSO (Jury 1993). The local response to an ENSO event is an increase in SSTs in the tropical Indian Ocean and an increase in subtropical westerly wind (Halpert and Ropelewski 1992), the former being favourable for TC formation and the latter not.

Waves in the easterlies are often a precursor to tropical cyclogenesis in the northern hemisphere. This mecha-

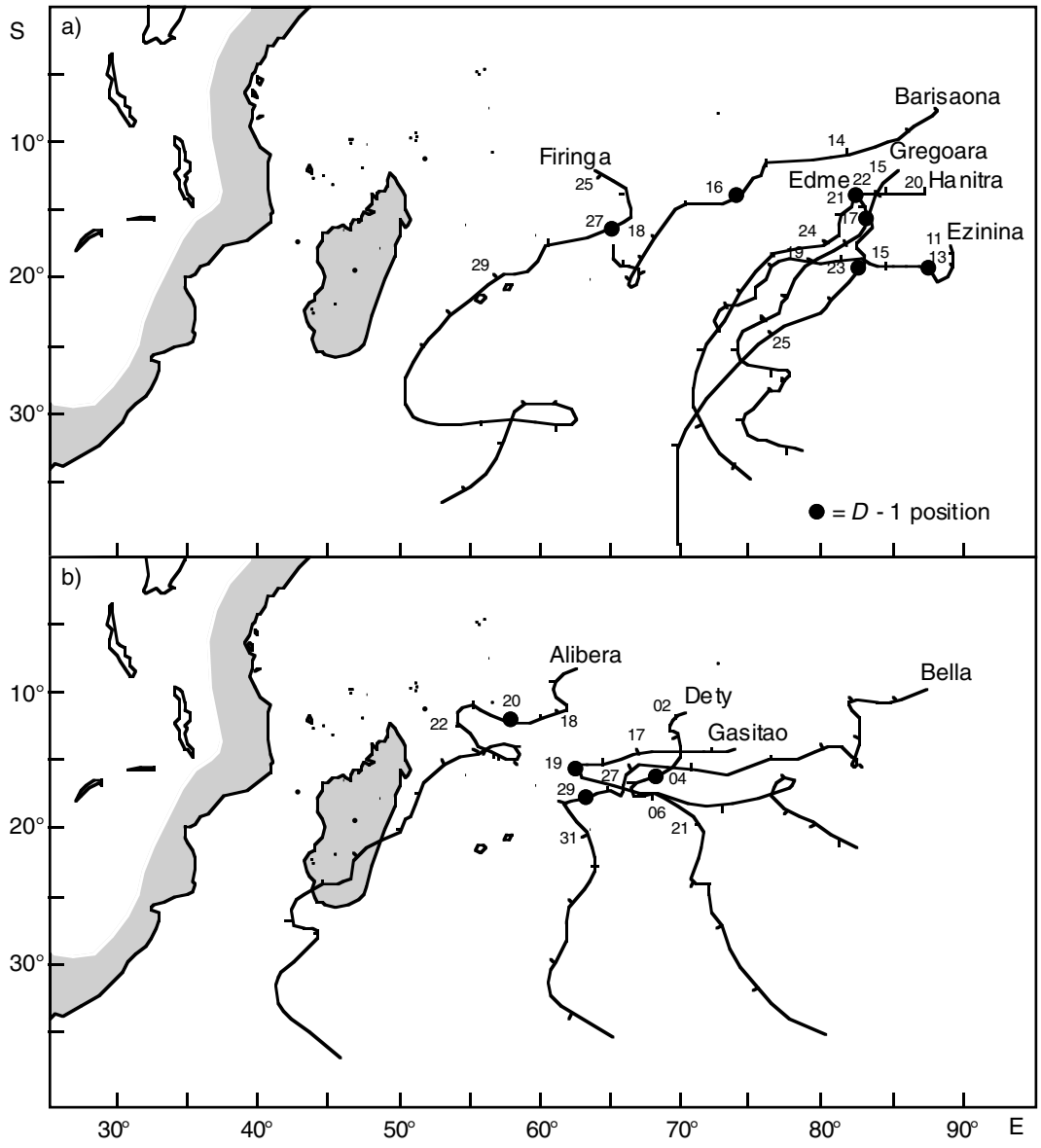

Fig. 2: TC tracks used to form (a) the westward-moving composites and (b) the recurving composites. Numbers refer to dates (see Table I) and tick marks show the daily positions

nism operates less frequently in the SW Indian Ocean (Padya 1989, Jury 1993, Jury *et al.* 1994). Transient barotropic waves of the SW Indian Ocean exhibit a wide variety of structure and are slower and less coherent than in other tropical cyclogenesis regions (Jury *et al.* 1991). TC track and intensity, and interaction with the background circulation have become a focal point of interest.

Tropical cyclone prediction in the SW Indian Ocean is still in its infancy, compared to other regions.

Vermeulen and Jury (1992) assessed the precision of TC model forecasts by comparing track predictions from the UK Meteorological Office (UKMO) model with observations for the period 1989–1991. The authors found that track prediction up to three days before maximum intensity ($D-3$) was adequate, with errors >500 km thereafter. Initial TC placement errors were found, on average, to be 172 km and often compounded in subsequent forecasts (Pathack 1997). Problems were encountered when TCs moved across mountainous Madagascar. The inconsistency of forecast errors was attributed to parameterization problems, which have been partially rectified (Heming *et al.*1995). Predictability in the SW Indian Ocean region was found to be complicated by low-frequency surges of the north-west monsoon (Wang and Rui 1990), the absence of background easterly flow in the 500–300 hPa layer, the irregular nature of easterly waves, and a lack of upper-level observations near the intertropical covergence zone (ITCZ) over the central ocean basin. A positive attribute found was the ability of the UKMO model to predict TC genesis in response to upper-level dynamic forcing.

In this study, composites are made of the kinematic and thermodynamic environment for westward-moving and poleward-recurving TCs in order to address the following questions:

(i) What synoptic-scale features in the circulation and thermodynamic fields distinguish track characteristics?
(ii) How do the synoptic meteorological fields evolve as the TC intensifies?
(iii) What are the physical processes underlying TC development in the SW Indian Ocean?

The study also aims to establish whether a substantial difference in the structure of the surrounding atmospheric envelope distinguishes the two TC types; and whether knowledge of this can improve the prediction of cyclone tracks as an aid to early warning systems.

DATA AND METHODS

Meteorological data inputs to the European Community for Medium-Range Weather Forecasts (ECMWF) are briefly outlined, together with the primary and derived parameters. Procedures used to form means and composites are discussed. Meteorological studies frequently make use of model "enhanced" global datasets. These datasets are especially useful for studying the large-scale physical processes of the atmosphere in regions where conventional data acquisition is limited (Bengtsson and Shukla 1988). Some caution is advised when interpreting the finer detail of the results, because most data analyses, except operational TC track charts, originate from the ECMWF model.

ECMWF data

The ECMWF maintains a global atmospheric dataset, which began in 1979. The tropical analysis has benefited from diabatic initialization, creating more realistic and intense Hadley and Walker circulations. The introduction of the T106 Model in May 1985 resulted in more realistic temperature measurements from the tropics. Improvements have been noted with regard to satellite moisture observations and model representation of vertical uplift. Although satellite-retrieved data have enhanced knowledge of the tropospheric circulation, extrapolation is required to produce a gridded field. The study region is viewed by the Indian meteorological satellite, but operational inputs have been disappointing. Given the paucity of upper air observations, results here may be interpreted only for the synopticscale atmospheric environment in the SW Indian Ocean and its interaction with tropical cyclones.

ECMWF model analyses are reported here for the period 1986–1992, in the domain 25–100°E, 0–35°S. Although model products having a resolution of 1° are available, the processed model data used for this study had a resolution of 2.5°. This is appropriate considering the low density of the original observations. The six basic parameters obtained from ECMWF were: geopotential height, temperature, zonal wind component (u), meridional wind component (v), vertical motion (ω), and relative humidity at the levels 1 000, 850, 700, 500, 300, 200 and 100 hPa. Various parameters are illustrated at the most appropriate levels, i.e. vertical motion at 500 hPa, moisture variables below this level and divergence at 200 hPa.

Composite analysis technique

Where there is a scarcity of data available for the study of a specific weather phenomenon, compositing of multiple events with similar characteristics can often yield results superior to individual cases. Although the structure of individual cases is smoothed by compositing, this may be desirable because it eliminates small-scale peculiarities imposed by gaps in observations, among other factors. Compositing is particularly appropriate for regions where data are sparse, because it highlights common features. The

Table I: Dates of SW Indian Ocean tropical cyclones (TC) used in the westward-moving and recurving composites

Name	Date	*D* – 3	*D* – 1	*D* + 1
Westward-moving				
Ezinina	Feb. 1988	11	13	15
Barisaona	Nov. 1988	14	16	18
Edme	Jan. 1989	21	23	25
Firinga	Jan. 1989	25	27	29
Hanitra	Feb. 1989	20	22	24
Gregoara	Mar. 1990	15	17	19
Recurving				
Gasitao	Mar. 1988	17	19	21
Alibera	Dec. 1989	18	20	22
Dety	Feb. 1990	02	04	06
Bella	Jan. 1991	27	29	31

advantage is that many observations over a number of events can be accumulated, resulting in a more data-rich field, which can be averaged in a "TC-following" framework. Composites of various meteorological parameters can be compared, following stratification according to TC movement. Compositing has the effect of reducing geopotential gradients, tangential winds, vertical motion, upper level divergence, and low-level vorticity by 20–50% below that found in most individual cases.

The compositing procedure makes use of climatology and composite fields. The procedure for calculating TC composites is to average the spatial matrix for selected cases by grid point and pressure level each day and to divide by the sample size. The composite area is not fixed, but is system-following. Three days of TC activity are analysed around the time of maximum intensity. The day of maximum intensity (*D*-0) is defined as the day of maximum surface wind speed, following declaration of tropical cyclone status (based on a visible eye in satellite imagery) and a sustained surface wind >59 $m \cdot s^{-1}$. The two composite categories described here are the westward-moving and the poleward-recurving tropical cyclones. TCs are placed in a category according to the track followed by the cyclone from *D*-1 to *D*+1. Recurvature should occur early and not in the decaying phase when the TC is south of 20°S. Westward-moving TCs have a mean track of 230° at 3.7 $m \cdot s^{-1}$ and recurving cyclones move polewards 187° at 2.7 $m \cdot s^{-1}$. The compositing grid used in this study is a square with coordinates of 20° latitude × 20° longitude. Grid points are situated at every 2.5° latitude and longitude, resulting in a 9 × 9 point matrix, with the centre of the grid coincident with the estimated centre of the TC.

Table II: The positions and calculated mean centre of the westward-moving and recurving tropical cyclones in the SW Indian Ocean

Name	Position of centre		
	D – 3	*D* – 1	*D* + 1
Westward-moving TCs			
Ezinina	90°E, 10°S	87.5°E, 12.5°S	80°E, 12.5°S
Barisaona	80°E, 10°S	72.5°E, 12.5°S	67.5°E, 17.5°S
Edme	82.5°E, 15°S	82.5°E, 20°S	75°E, 25°S
Firinga	65°E, 12.5°S	65°E, 15°S	55°E, 20°S
Hanitra	85°E, 12.5°S	82.5°E, 12.5°S	80°E, 17.5°S
Gregoara	85°E, 12.5°S	82.5°E, 15°S	80°E, 20°S
Mean	82.5°E,12.5°S	80°E,15°S	72.5°E, 20°S
Mean (overall)	77.5°E,15°S		
Recurving TCs			
Gasitao	65°E, 15°S	62.5°E, 17.5°S	72.5°E, 22.5°S
Alibera	60°E, 10°S	57.5°E, 12.5°S	55°E, 12.5°S
Dety	70°E, 10°S	67.5°E, 15°S	67.5°E, 17.5°S
Bella	65°E, 17.5°S	62.5°E, 17°S	62.5°E, 20°S
Mean	65°E,12.5°S	62.5°E,15°S	75°E,17.5°S
Mean (overall)	65°E,15°S		

For each of the TC cases, the position of the centre was determined for each individual cyclone day (Table II). The position of the centre was obtained from the annual Mauritius tropical cyclone reports, the Reunion tropical cyclone reports and computer data records of SW Indian Ocean tropical cyclone track analysis (Appadu and Ragoonadeen, 1989a, b, 1990, Appadu and Goolaup 1991, Ecormier 1992). Figure 2 shows the tracks that individual TCs followed across the SW Indian Ocean during the study period.

After the individual grid data were extracted for each parameter, the average for each composite day was calculated. The statistical field significance was not evaluated, but intra-composite deviations were contributed relatively equally among the cases used. In addition to parameters being represented in the horizontal plane, those that exhibit interesting structure with height were analysed vertically along a meridional section through the composite TC centre. The mean TC composites for the westward-moving and the poleward-recurving cases were used to analyse structural evolution, and contrasts in the time from *D*-3 to *D*+1. Recognized kinematic, thermodynamic and moisture patterns in the surrounding synoptic-scale atmospheric environment can be incorporated into conceptual models for operational forecast purposes.

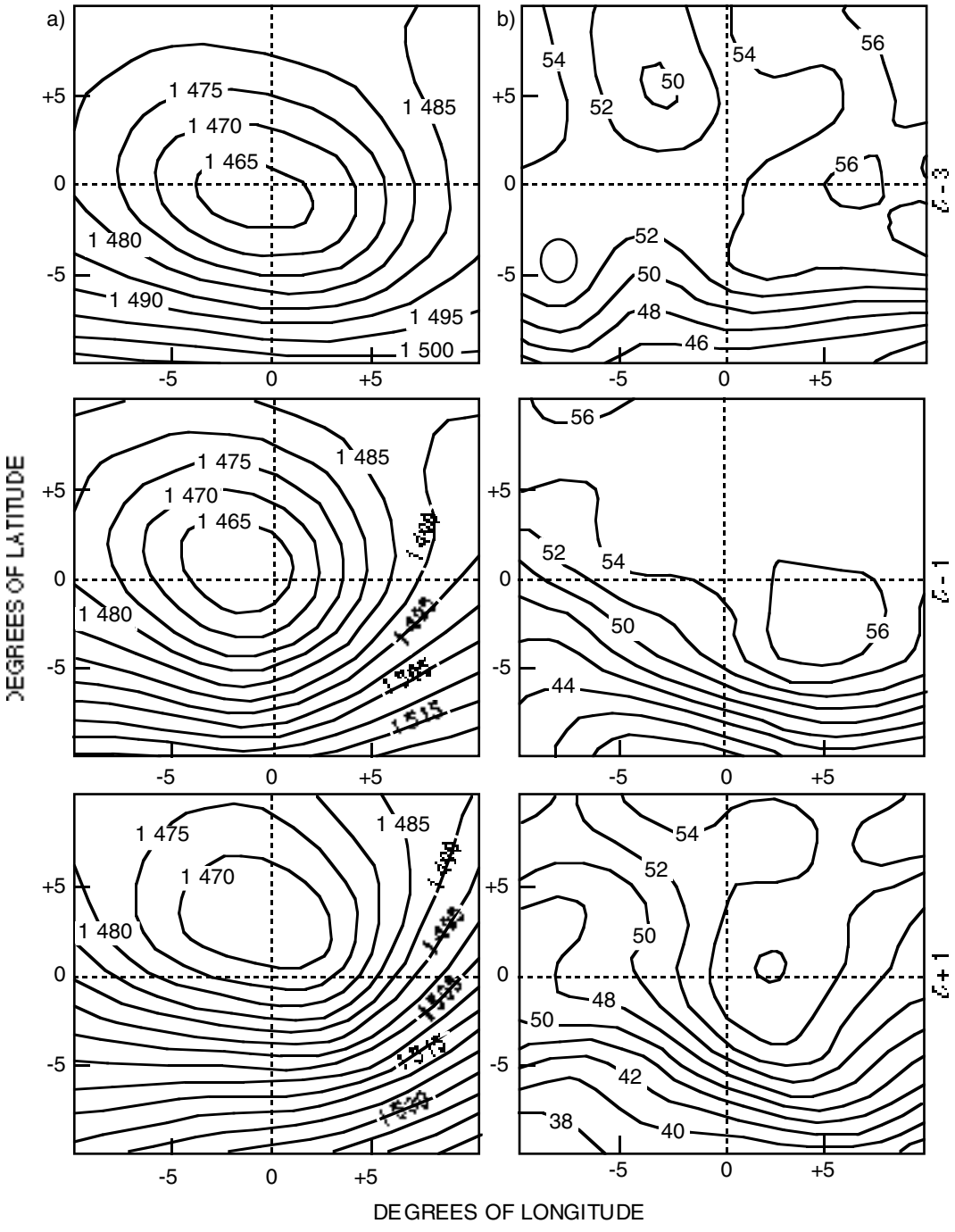

Fig. 3: (a) Westward-moving TC geopotential sequence at 850 hPa (contour interval is 5 gpm); (b) precipitable water field between the surface and 300 hPa (contour interval is 1 mm)

RESULTS

The results focus on environmental features surrounding composite tropical cyclones. Mean horizontal and vertical sections have been used to analyse the various ECMWF observed parameters. Six SW Indian Ocean TCs whose tracks were orientated towards the south-west were formed into the westward-moving composite and four TCs whose tracks changed to the south-east were used to form the recurving composite (Tables I and II).

Westward-moving TC analyses

A steady concentric pattern characterizes the low-level geopotential field (Fig. 3a). The 850 hPa geopotential minimum remains in the range 1 465–1 470 gpm and undergoes a relative north-westward shift away from the centre-point throughout the sequence. Figure 3b describes precipitable water patterns and illustrates values >54 mm to the north-east. To the south, precipitable water contours are zonal with a steep decline. On *D*-1, the region of high values to the east of the TC centre increases to >57 mm. On *D*+1, values <38 mm are to the south-west of the TC centre. The pattern rotates clockwise through the sequence. The precipitable water field shows a steep gradient for values <52 mm throughout the sequence, particularly polewards of the TC, as expected.

Winds at 850 hPa show the expected cyclonic structure (Fig. 4a). Although a relatively symmetrical pattern is maintained throughout the sequence, winds increase in the south-west quadrant by *D*+1. Speeds are around 10 $m \cdot s^{-1}$, indicative of the inability of low-resolution model products to capture TC structure. Low-level cyclonic vorticity values remain near $-3 \times 10^{-5} \cdot s^{-1}$ throughout the sequence. The wind at 200 hPa exhibits some evolution (Fig. 4b). On *D*-3, easterly flow is maintained to the north (>10 $m \cdot s^{-1}$). By *D*-1, upper westerly winds in the south-west quadrant have increased in magnitude to >15 $m \cdot s^{-1}$. A change is seen on *D*+1, where the magnitude of north-westerly winds in the south-western half of the composite has increased and extended northwards to the centre-point.

Meridional vertical section analyses (westward-moving cyclones)

Meridional sections of the synoptic environment are analysed for 10° latitude either side of the estimated position of the composite TC. The equator (north) is to the left in these panels. The meridional divergence section shows a progressive decline in strength of the upper level divergence (Fig. 5a). On *D*-3, the maximum divergence of $6 \times 10^{-5} \cdot s^{-1}$ is located in the southern sector at 200 hPa, whereas at the surface, convergent flow reaches a maximum of $-9 \times 10^{-5} \cdot s^{-1}$. The strength of the surface convergence, as well as divergence at 200 hPa, has diminished by *D*-1. Although the surface convergence is still present on *D*+1, the upper level divergence has decreased to $2 \times 10^{-5} \cdot s^{-1}$. Most noteworthy is the shallowness of the surface convergence; values $<-2 \times 10^{5} \cdot s^{-1}$ are confined below 850 hPa.

Throughout the sequence, an area of cyclonic vorticity (negative) is dominant, as expected for TCs (Fig. 5b). On *D*-3, cyclonic vorticity extends through the troposphere, with a maximum of $-2.5 \times 10^{-5} \cdot s^{-1}$ below 700 hPa. The area of cyclonic vorticity $<-2.5 \times 10^{-5} \cdot s^{-1}$ reaches up to 500 hPa on *D*-1, with lower values at 850 hPa. On *D*+1, anticyclonic vorticity appears to dominate the sector south of the TC centre, with a value of $>2 \times 10^{-5} \cdot s^{-1}$ between 500 and 200 hPa. An equatorward tilt is evident in the cyclonic vorticity minima.

The vertical structure of equivalent potential temperature (θe) is shown in Figure 6a. Maximum lapse rates for θe occur on the equatorward side of the TC in the 850 hPa layer, whereas the poleward edge remains relatively stable through the sequence. On *D*-3, a minimum area of <330 K is situated across the TC centre above 700 hPa, with a maximum of >350 K at the surface. On both *D*-1 and *D*+1, the 330 K minimum is located in the south. Surface instability is signalled by θe >350 K. During the sequence, surface θe in the southern sector (+5° latitude) declines progressively. This change is noteworthy because it occurs along the TC track. Dry air is available for entrainment on the poleward side in the 700–600 hPa layer, whereas subsident outflow is on the equatorward side.

The sequence of vertical motion shows a reduction in the strength of vertical upward motion (Fig. 6b). The core of uplift on *D*-3 is situated in the southern sector from the surface to 100 hPa. The area of strongest upward motion of <-1.4 $Pa \cdot s^{-1}$ is found near 400 hPa, located 2.5° south of the centre-point. On *D*-1, convective uplift in the southern rim is reduced to -0.8 $Pa \cdot s^{-1}$. Downward motions are between 5 and 7.5° latitude north of the centre-point. By *D*+1, the uplift weakens further to <-0.4 $Pa \cdot s^{-1}$ and becomes shallower.

Recurving TC analyses

The synoptic environment surrounding tropical cy-

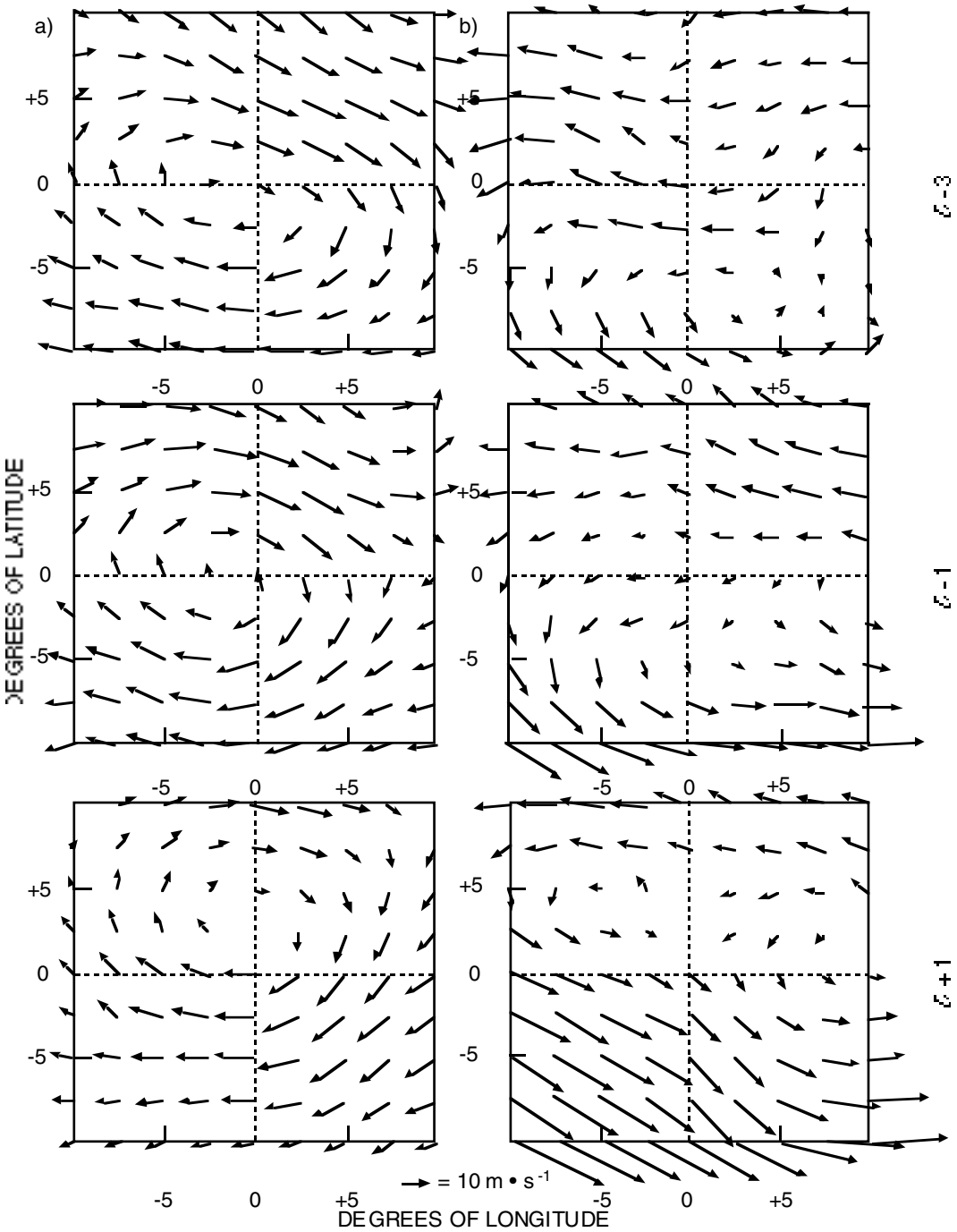

Fig. 4: Westward-moving TC horizontal wind field at (a) 850 hPa and (b) 200 hPa

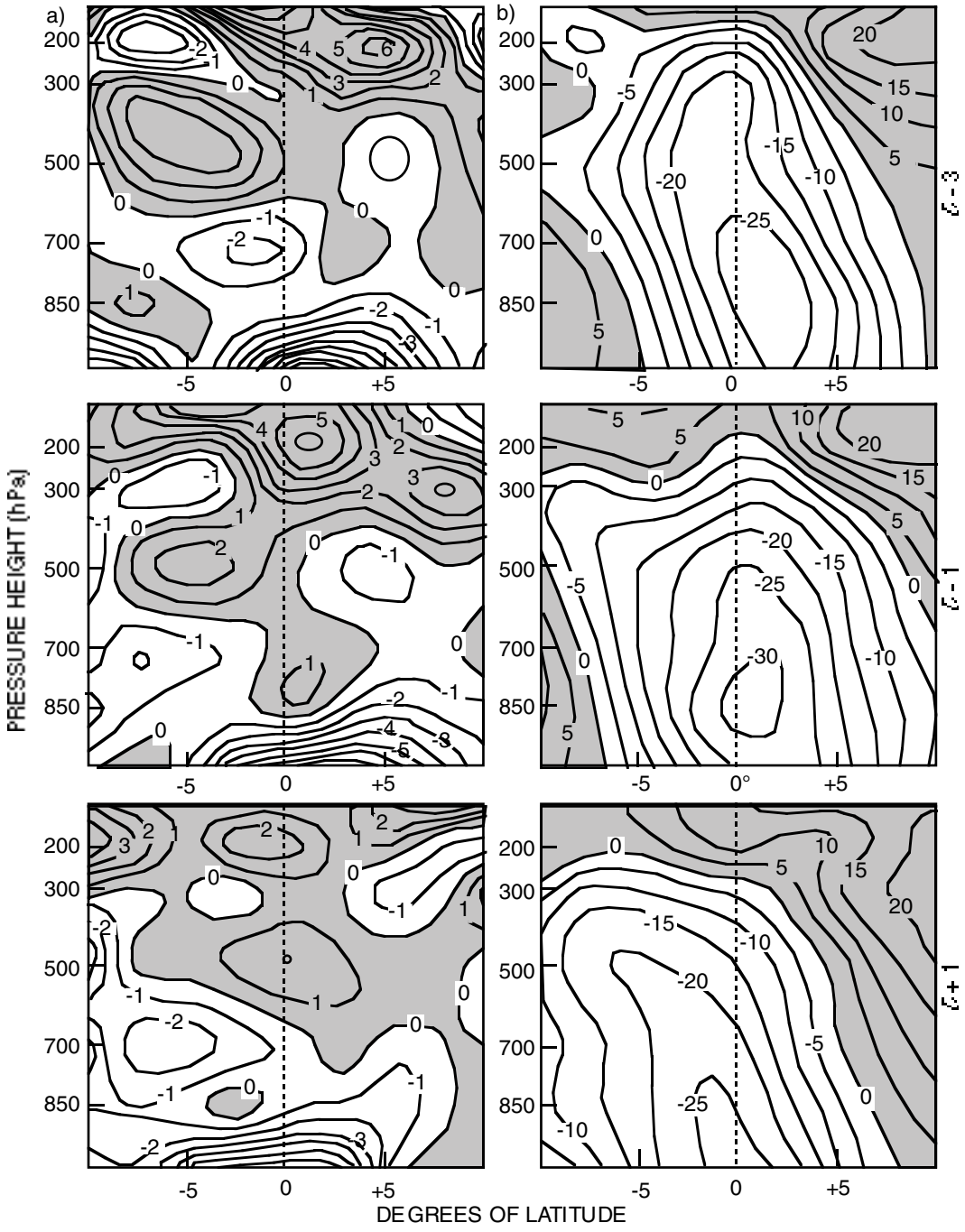

Fig. 5: Westward-moving TC meridional section of (a) divergence field (contour interval is $1 \times 10^{-5} \cdot s^{-1}$) and (b) vorticity field (contour interval is $5 \times 10^{-6} \cdot s^{-1}$). Equatorward is to the left

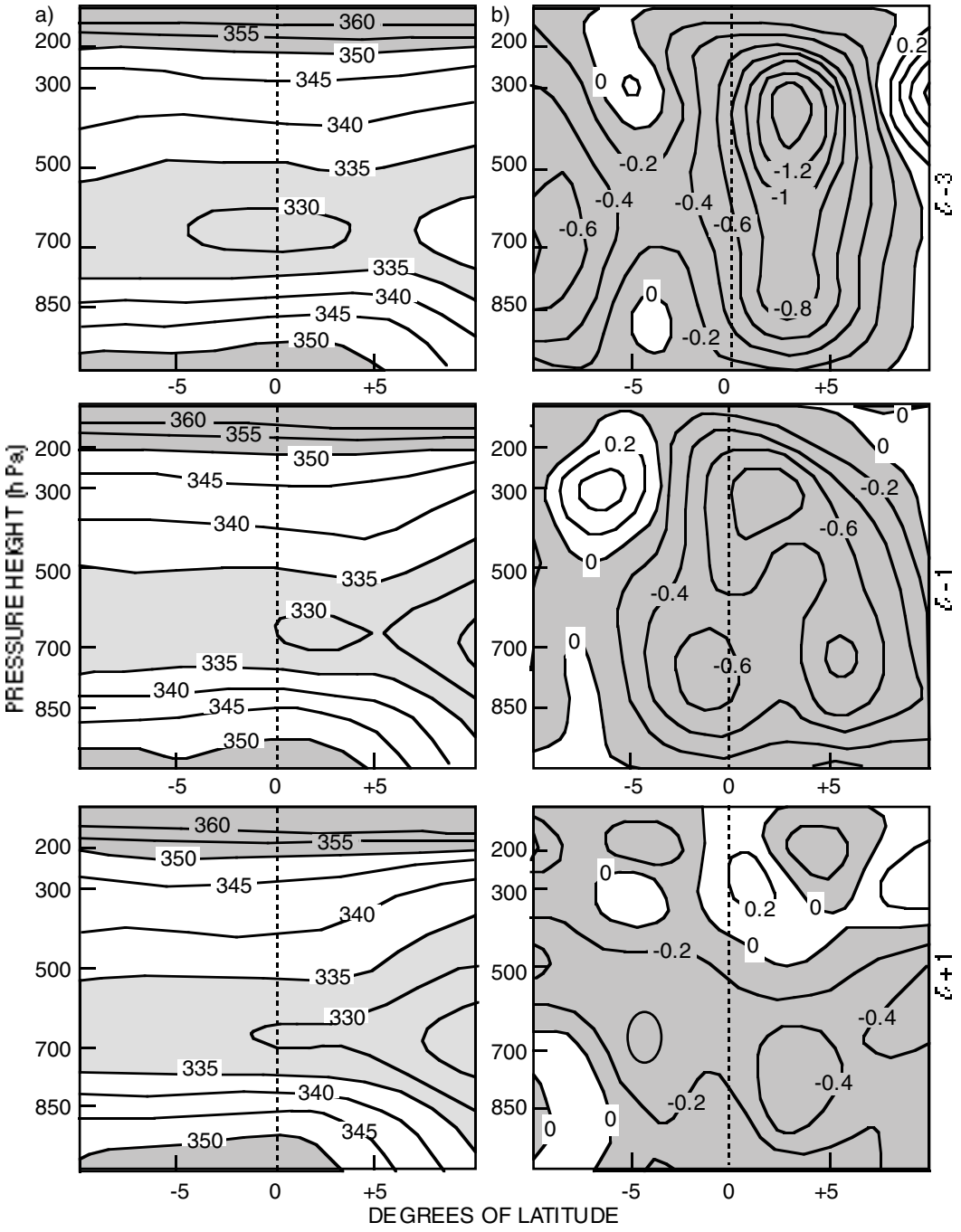

Fig. 6: Westward-moving TC meridional section of (a) equivalent potential temperature (contour interval is 5°K) and (b) vertical motion field (contour interval is 0.1 Pa·s^{-1}). Equatorward is to the left

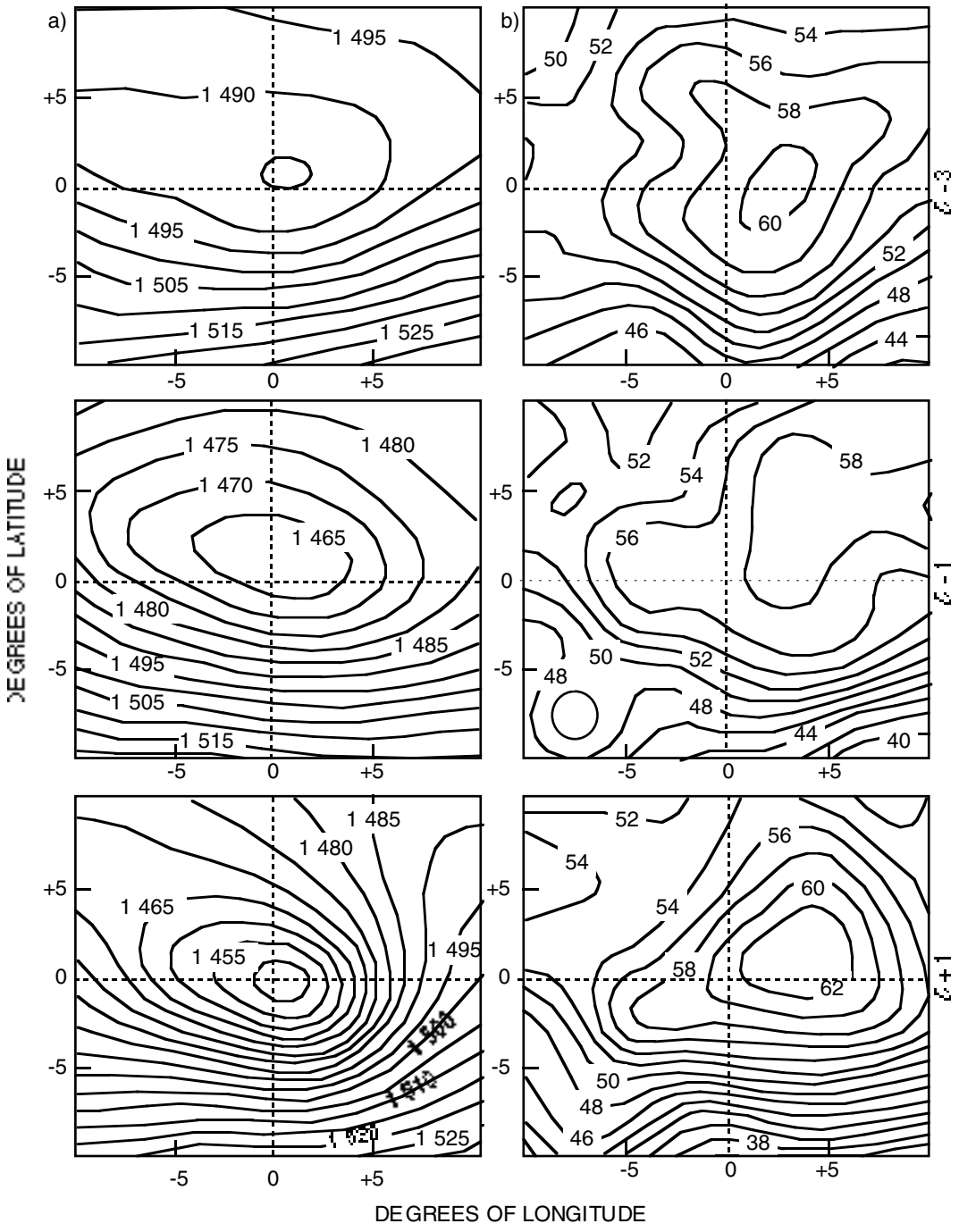

Fig. 7: (a) Recurving TC geopotential sequence at 850 hPa (contour interval is 5 gpm), (b) precipitable water field between the surface and 300 hPa (contour interval is 1 mm)

clones that exhibit a recurving track is described by the following analyses. The 850 hPa geopotential minimum intensifies during the sequence (Fig. 7a), when the minimum goes from 1 485 to 1 450 gpm. The gradients become particularly strong to the south, in the direction of motion.

The precipitable water initially declines then increases throughout the sequence (Fig. 7b). On *D*-3, a region of high precipitable water (>60 mm) is situated east of the centre. Precipitable water values decrease away from this maximum, especially polewards. A minimum of <44 mm is located in the south-east. *D*-1 exhibits a decrease of 2 mm in the maximum precipitable water value and a shift towards the north-east. By *D*+1, precipitable water increases to >62 mm, a value about 10% higher than for the westward-moving composite. In the southern sector, values decrease to <36 mm.

Low-level winds do not describe the expected cyclonic vortex, in comparison with the westward-moving TC (Fig. 8a), and point to deficiencies in data assimilation and model analysis. On *D*-3, higher wind speeds of around 10 $m \cdot s^{-1}$ are found in the southern sector, in contrast to the northern sector with speeds of <5 $m \cdot s^{-1}$. The winds are largely zonal in both *D*-3 and *D*-1 composites and do not form a vortex around the centre. On *D*-1, the zonal pattern of winds remains, but monsoon westerly winds increase near the equator. A strong cyclonic rotation is only evident on *D*+1, when the winds in the south-eastern quadrant exhibit a marked north-easterly component, with wind speeds >10 $m \cdot s^{-1}$. The low-level cyclonic vorticity increases in intensity during the composite sequence, from -2 to $-3 \times 10^{-5} \cdot s^{-1}$. Upper winds display a consistent pattern of westerlies in the south (Fig. 8b). Initial easterly flow in the tropics is replaced by westerly winds of speeds >12 $m \cdot s^{-1}$ by *D*-1. A mid-latitude intrusion is evident as westerly wind speeds increase to >20 $m \cdot s^{-1}$ in the south-east on *D*+1. It is not surprising that the TC recurves under these westerly wind conditions.

Meridional vertical section analyses (recurving cyclones)

Meridional sections of the synoptic environment are composited for 10° latitude either side of the estimated centre of recurving TCs. The divergence section reveals changes in structure at 200 hPa (Fig. 9a). On *D*-3, two regions of divergence > $+4 \times 10^{-5} \cdot s^{-1}$ are found either side of the centre at 200 hPa. At the surface, the convergence attains a strength of $< -6 \times 10^{-5} \cdot s^{-1}$. On *D*-1, there is a single area of upper divergence ($+6 \times 10^{-5} \cdot s^{-1}$). The surface convergence remains $< -6 \times 10^{-5} \cdot s^{-1}$ and is more confined. By *D*+1, there is a significant increase in surface convergence and upper divergence.

Deep cyclonic vorticity around the centre is evident in Figure 9b. Penetration of cyclonic vorticity to 200 hPa and a two-fold increase in the gradient between the cyclonic and the anticyclonic vorticity regions takes place from *D*-3 to *D*+1. This signifies that increasing latitude (e.g. coriolis) modulates the TC structure. Maximum cyclonic vorticity is at 850 hPa, and increases to $< -5.5 \times 10^{-5} \cdot s^{-1}$ by *D*+1. The region of anticyclonic vorticity at 200 hPa south of the centre maintains a value $> +1 \times 10^{-5} \cdot s^{-1}$ from *D*-3 to *D*+1.

There is little change in equivalent potential temperature on the equatorward side of the composite recurving TC, whereas it is markedly reduced on the southern side (Fig. 10a). The upper-level lapse rate is unchanged with time and θe increases towards the tropopause. A minimum equivalent potential temperature (<330 K) is located on the southern fringe at 700 hPa. Closure of the 340 K isoline through the sequence is indicative of vigorous convective mixing to saturation. This pattern is unlike the westward-moving composite, where a relatively low equivalent potential temperature remains over the centre.

The dominant feature of the vertical motion field is the growth observed in the uplift region over and just south of the system's centre from -1 $Pa \cdot s^{-1}$ on *D*-3 to -2.6 $Pa \cdot s^{-1}$ on *D*+1 (Fig. 10b). Uplift reaches a maximum following recurvature of the composite TC towards the south-east. On *D*-3, two areas of high uplift (< -0.6 $Pa \cdot s^{-1}$) are on either side of the centre-point, whereas a region of low uplift is found over the centre-point. The uplift region coalesces in the 850–400 hPa layer, with values < -1.0 $Pa \cdot s^{-1}$. From *D*-1 to *D*+1, the uplift region near the centre of the TC increases by a factor of two, resulting in steep gradients.

DISCUSSION

An analysis of the synoptic-scale atmospheric envelope surrounding tropical cyclones in the SW Indian Ocean has been conducted using ECMWF model data. The large-scale environment supports a coherent vortex throughout the sequence in the westward-moving TC case. The geopotential height, horizontal wind, vertical motion, divergence and vorticity decrease slightly in strength, signalling TC decay. For the poleward-recurving TC composite, large-scale environmental conditions are conducive

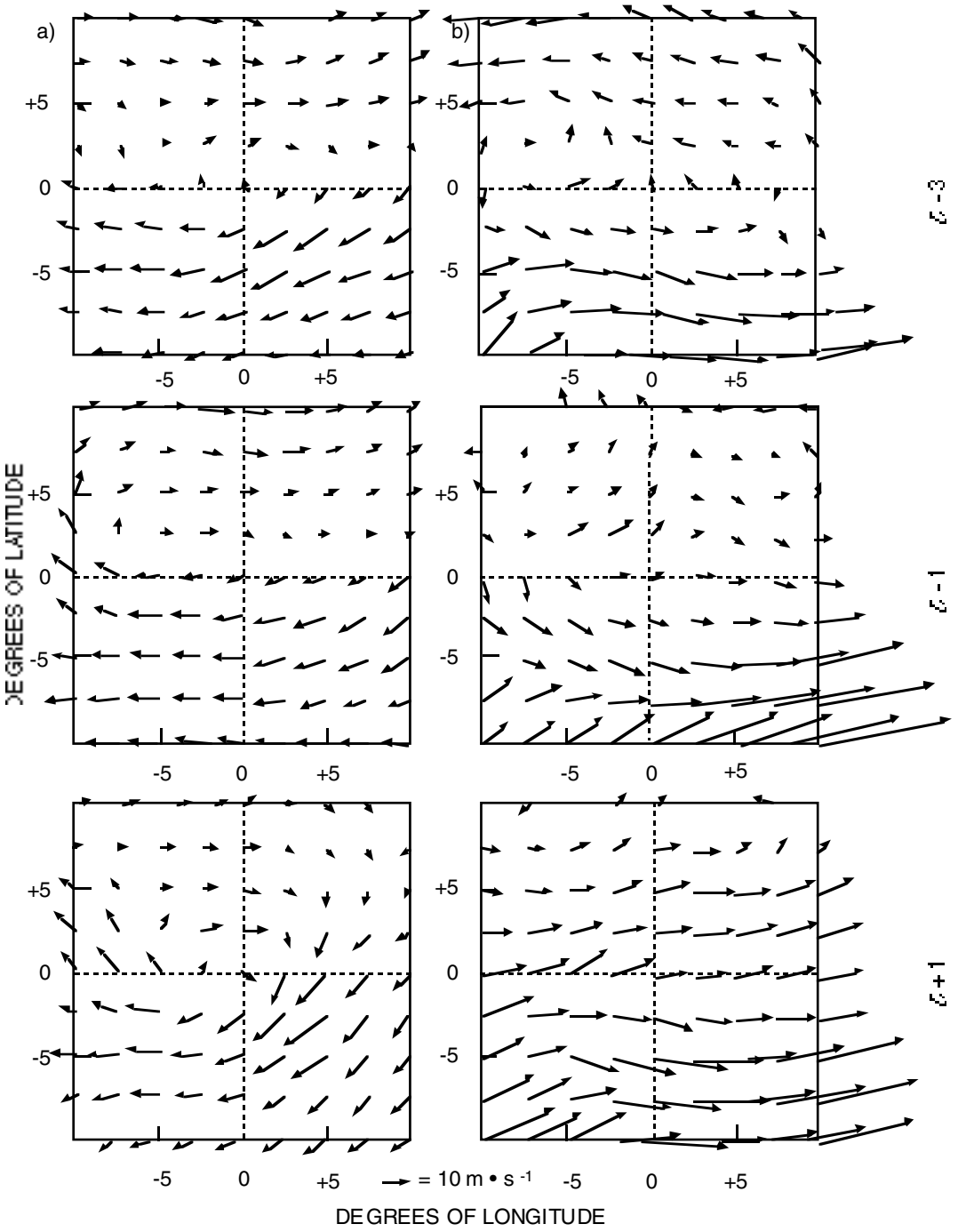

Fig. 8: Recurving TC horizontal wind field at (a) 850 hPa and (b) 200 hPa

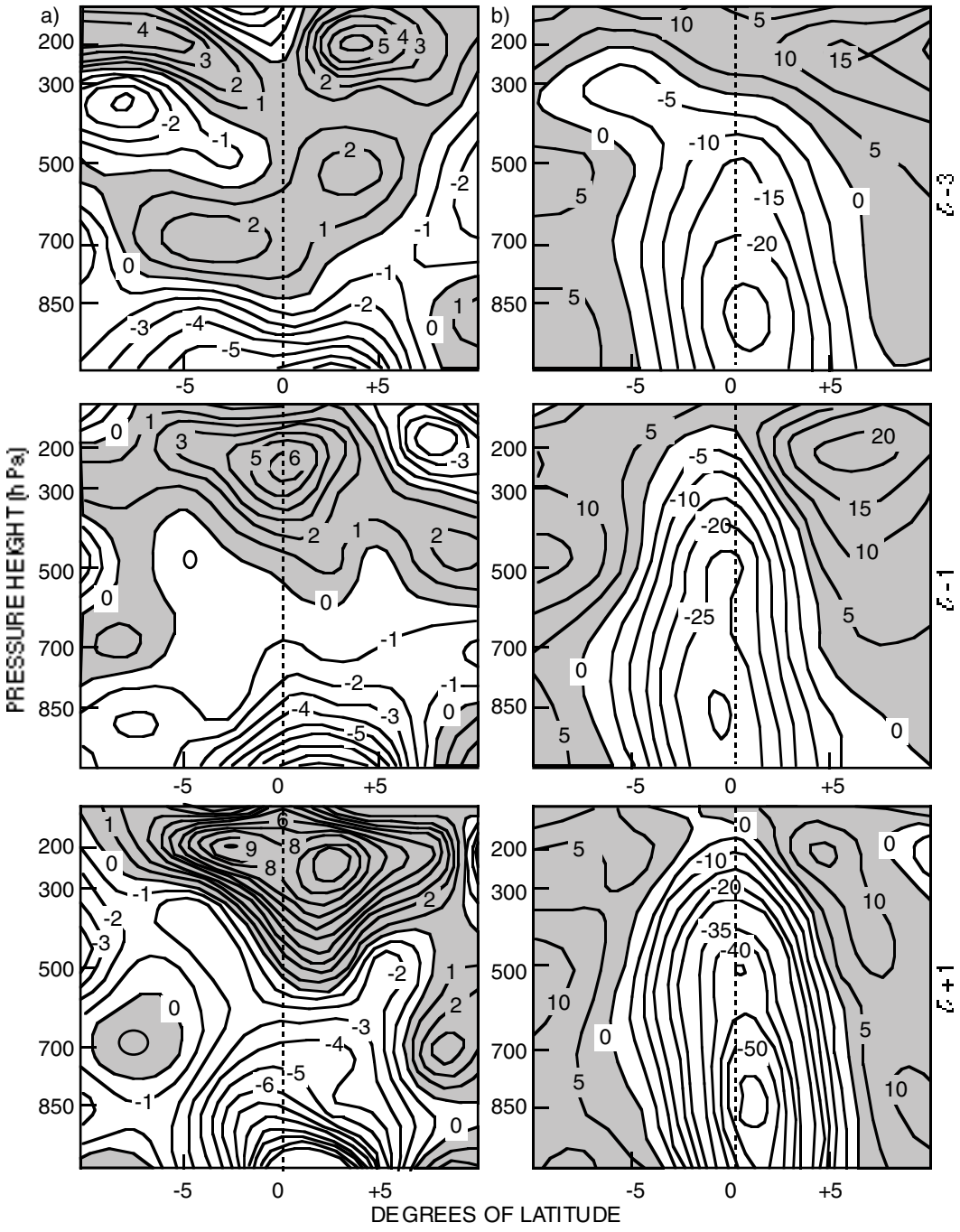

Fig. 9: Recurving TC meridional section of (a) divergence field (contour interval is $1 \times 10^{5} \cdot s^{-1}$) and (b) vorticity field (contour interval is $5 \times 10^{-6} \cdot s^{-1}$). Equatorward is to the left

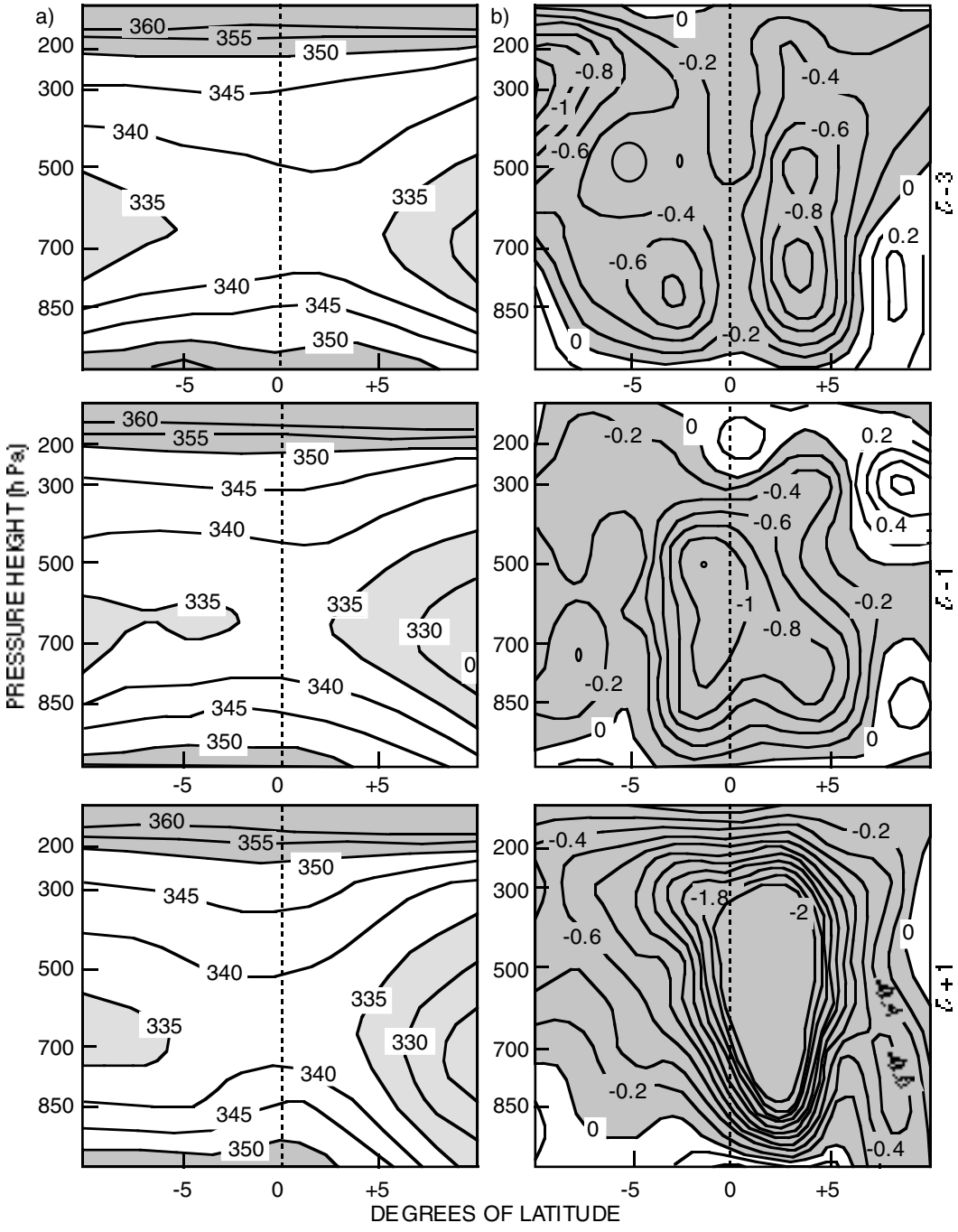

Fig. 10: Recurving TC meridional section of (a) equivalent potential temperature field (contour interval is 5°K) and (b) vertical motion field (contour interval is 0.1 Pa·s^{-1}). Equatorward is to the left

Table III: Guidelines to distinguish potential tropical cyclone track in ECMWF model analyses

Parameter	Westward-moving tropical cyclone	Recurving tropical cyclone
Geopotential	P_{850} min : 1 465 gpm on $D-3$ P_{200} min : 12 450 gpm on $D+1$	P_{850} min : 1 450 gpm on $D+1$ P_{200} min : 12 455 gpm on $D-3$
	WM weakens, REC strengthens	
Horizontal wind	P_{850} max : > 10 m·s^{-1} on $D-3$ P_{200} max : > 15 m·s^{-1} on $D+1$	P_{850} max : 10 m·s^{-1} on $D+1$ P_{200} max : > 23 m·s^{-1} on $D-1$
	Cyclonic structure for WM, strong winds shift NE to SE Cyclonic structure for REC, only on $D+1$ Upper westerlies in front of WM	
Kinetic energy	P_{850} max : 70 J·kg^{-1} on $D-1$ P_{200} max : 280 J·kg^{-1} on $D+1$	P_{850} max : 100 J·kg^{-1} on $D+1$ P_{200} max : >300 J·kg^{-1}on $D+1$
	Strength doubles for REC, $D-3$ to $D+1$	
Vertical motion	P_{500} max : –1.2 Pa·s^{-1} on $D-3$	P_{500} max : –3 Pa·s^{-1} on D+1
	Decreases for WM, REC intensity increases 3-fold	
Upper divergence	P_{200} max : $+8 \times 10^{-5}$·s^{-1} on $D-3$	P_{200} max : $+10 \times 10^{-5}$·s^{-1} on $D+1$
	WM decreases, REC increases	
Vorticity	P_{850} max : -30×10^{-5}·s^{-1} on $D-1$ P_{200} max :$+30 \times 10^{-5}$·s^{-1}	P_{850} max : -40×10^{-5}·s^{-1} on $D+1$ P_{200} max :$+20 \times 10^{-5}$·s^{-1} on $D-1$
	Increased low-level cyclonic vorticity for REC Constant for WM upper anticyclonic vorticity Increased depth for REC, equatorward tilt for WM	
Precipitable water	Max : 57 mm on $D-1$	Max : 62 mm on $D+1$
	REC areal extent larger, input from east	
Equivalent potential temperature	P_{850} max : 346 K on $D-1$ P_{500} max : 337 K on $D-1$	P_{850} max : 346 K on $D+1$ P_{500} max : 341 K on $D+1$
	Constant for WM and REC Upper level REC higher than WM	
Synthesis	Upper level trough acts as an "attractor", WM steady, REC intensifying	

WM = Westward-moving
REC = Recurving

to vortex development. The value and gradient of most parameters increases from D-1 to D+1, partly because of conservation of absolute vorticity (e.g. increasing latitude). The presence of strong westerly winds in the upper troposphere, recognized as a condition for TC recurvature (Hodanish and Gray 1993), appears to be a dominant feature in this study.

Differences between the composite TC environments for westward-moving and recurving cases are outlined in Table III. These characteristics can be used in the operational environment to improve short-term predictability of TC tracks. Both composite TC centres shift polewards by >10° latitude during the sequence, resulting in an increased solenoidal effect in the vorticity budget. Because background easterly flow is weak, subtropical troughs situated over Madagascar may attract and enhance SW Indian Ocean TCs, more so than has been seen in other TC regions. The results indicate that the westward-moving TCs are thermally driven, whereas the recurving TCs are dynamically driven.

Previous research on TC recurvature has shown that tropospheric winds poleward of cyclones are important. George and Gray (1976) showed that changes in zonal flow produce noticeable changes in track. Penetration of upper-westerly flow 6–10° polewards and west of

the cyclone centre increases as the TC starts to recurve in the NW Pacific. In the SW Indian Ocean, upper troughs in the more persistent extra-tropical westerly flow alter TC track. Upper westerly winds polewards of the centre enhance development of the recurving TC through the creation of effective anticyclonic outflow for mass overturning.

Although a limited number of cases were used here in the production of the TC composites, there is a potential for using these results for improved short-term forecasting. Studies of individual destructive TC events using more direct sources of information, such as satellite-microwave rainfall rate and scatterometer winds, longer time sequences and higher resolution model analyses could be undertaken to investigate how the large-scale atmospheric circulation adjusts to and governs TC intensification and track changes in the SW Indian Ocean.

ACKNOWLEDGEMENTS

We thank Mr K. M. Levey (University of Virginia, USA), who assisted with data programming, and Mr A. Nassor (Madagascar Meteorological Service) and Dr A. Makarau (University of Zimbabwe), who offered useful advice. The Foundation for Research Development Dynamics of Marine Weather Systems Project supported this research, which was conducted at the Oceanography Department, University of Cape Town.

LITERATURE CITIED

ANYAMBA, E. K., KIANGA, P. M. R. and J. K. PATNIAK 1982 — The mean horizontal motions over the African atmosphere during the southern summer. *Proc. tech. Conf. Clim. Afr. WMO 596, Tanzania*: 158–170.

APPADU, S. N. S. and P. GOOLAUP 1991 — Cyclone season of the SW Indian Ocean 1990–1991. Techical Report **CS 14**, Mauritius Meteorological Services, Vacoas, Mauritius: 32 pp. + Appendix.

APPADU, S. N. S. and S. RAGOONADEEN 1989a — Cyclone season of the SW Indian Ocean 1987–1988. Techical Report **CS 11**, Mauritius Meteorological Services, Vacoas, Mauritius: 27 pp. + Appendix.

APPADU, S. N. S. and S. RAGOONADEEN 1989b — Cyclone season of the SW Indian Ocean 1988–1989. Techical Report **CS 12**, Mauritius Meteorological Services, Vacoas, Mauritius: 23 pp. + Appendix.

APPADU, S. N. S. and S. RAGOONADEEN 1990 — Cyclone season of the SW Indian Ocean 1989–1990. Technical Report **CS 13**, Mauritius Meteorological Services, Vacoas, Mauritius: 31 pp. + Appendix.

ARKIN, P. A., KONSKY, V. E., JANOWIAK, J. E. and E. A. O'LENIC 1986 — Climate Analysis Center NOAA Atlas 7, *Nat. Met. Center*, *Washington DC*: 8 pp. + 85 Figures.

BENGSSTON, L. and J. SHUKLA 1988 — Integration of space and *in situ* observations to study global climate change. *Bull. Am. met. Soc*. **69** (10): 1130–1143.

DENNET, M. D. 1978 — Variations of rainfall and seasonal forecasting in Mauritius. *Arch. Met. Geophys. Biokl*. **B25**: 359–370.

ECORMIER, J. 1992 — *Cyclones Tropicaux du Sud-ouest de l'Ocean Indien*. Meteo France; Réunion Meteorological Service: 480 pp.

GEORGE, J. E. and W. M. GRAY 1976 — Recurvature and non-recurvature as related to surrounding wind/height fields, *J. appl. Met*. **16**: 34–42.

GRAY, W. M. 1984 — Atlantic seasonal hurricane frequency. 1. *El Niño* and 30 mb quasi-biennial oscillation influences. *Mon. Weath. Rev*. **112**: 1649–1668.

HALPERT, M. S. and C. F. ROPELEWSKI 1992 — Surface temperature patterns associated with the Southern Oscillation. *J. Climatol*. **5**: 577–593.

HASTENRATH, S. 1985 — *Climate and Circulation of the Tropics*. Dordrecht; Reidel: 455 pp.

HEMING, J. T., CHAN, J. C. L. and A. M. RADFORD 1995 — A new scheme for the initialisation of tropical cyclones in the UKMO global model. *Met. Applic*. **2**: 17–184.

HODANISH, S. and W. M. GRAY 1993 — An observational analysis of tropical cyclone recurvature. *Mon. Weath. Rev*. **121**: 2665–2689.

JURY, M. R. 1992 — A climate dipole governing the interannual variability of convection over the SW Indian Ocean and SE Africa region. *Trends geophys. Res.* **1**: 165–172.

JURY, M. R. 1993 — A Preliminary study of climatological associations and characteristics of tropical cyclones in the SW Indian Ocean. *Met. atmos. Phys.* **51**: 101–115.

JURY, M. R., PARKER, B. and D. WALISER 1994 — Evolution and variability of the ITCZ in the SW Indian Ocean: 1988–90. *Theor. appl. Climatol*. **48**: 187–194.

JURY, M. R. and B. PATHACK 1991 — A study of climate and weather variability over the tropical southwest Indian Ocean. *Met. atmos. Phys*. **47**: 37–48.

JURY, M. R., PATHACK, B., CAMPBELL, G., WANG, B. and W. LANDMAN 1991 — Transient convective waves in the tropical SW Indian Ocean. *Met. atmos. Phys*. **47**: 27–36.

MARTIN, D. W., HINTON, B. B. and B. A. AUVINE 1993 — Three years of rainfall over the Indian Ocean. *Bull. Am. met. Soc*. **74**: 581–590.

PADYA, B. M. 1989 — *Weather and Climate of Mauritius*. Port Louis, Maritius; Mahatma Gandhi Institute: 283 pp.

PATHACK, B. M. R. 1993 — Modulation of South African summer rainfall by global climatic processes. Ph.D. thesis, University of Cape Town: 325 pp.

PATHACK, B. M. R. 1997 — On bogusing and tracking tropical cyclones: a case study. In *Proceedings of the 5th International Conference of the southern Hemisphere. Meteorology Ocean,Pretoria. Am. met. Soc.*: 134–135.

VERMEULEN, J. H. and M. R. JURY 1992 — Tropical cyclones in the south-west Indian Ocean – track prediction and verification 1989–91. *Met. Mag*. **121**: 186–192.

WALKER, N. D. 1989 — Sea surface temperature-rainfall relationships and associated ocean-atmosphere coupling mechanisms in the southern African region. Ph.D. thesis, University of Cape Town: 173 pp.

WANG, B. and H. RUI 1990 — Synoptic climatology of transient intraseasonal convection anomalies: 1975–1985. *Met. atmos. Phys.* **44**: 43–61.

WILLIAMS, J. B. 1990 — Some temporal and regional variations of climate in Madagascar. *Tech. Rep. Overseas Dev. Nat. Res. Inst., Chatham Marine, Kent*: 144 pp.